

Supporting Information

Achieving highly efficient catalysts for hydrogen evolution reaction by electronic state modification of platinum on versatile $\text{Ti}_3\text{C}_2\text{T}_x$ (MXene)

Youyou Yuan[†], *Haisheng Li*[†], *Ligang Wang*[†], *Lei Zhang*[†], *Dier Shi*[†], *Yuexian Hong*[†] and *Junliang Sun*^{†,*}

[†] College of Chemistry and Molecular Engineer, Peking University, Beijing National Laboratory for Molecular Sciences(BNLMS), 5 Yiheyuan Road, Beijing, 100871, PR China.

* Corresponding Author, Email: junliang.sun@pku.edu.cn (Junliang Sun)

Table of contents (9 pages)

Figure S1 Morphological characterization of $\text{Ti}_3\text{C}_2\text{T}_x$	S2
Figure S2 XRD patterns of TBA- $\text{Ti}_3\text{C}_2\text{T}_x$ treated with different TBAOH solution	S2
Figure S3 TEM characterization of D- $\text{Ti}_3\text{C}_2\text{T}_x$	S2
Figure S4 Morphological characterization of TBA- $\text{Ti}_3\text{C}_2\text{T}_x$	S3
Figure S5 Morphological characterization of the supports and the catalysts	S3
Figure S6 Optimization results of TBA- $\text{Ti}_3\text{C}_2\text{T}_x$ -Pt in the reduction with NaBH_4	S4
Figure S7 XRD patterns of the catalysts obtained by the UV-induced method	S4
Figure S8 XPS results of the catalysts	S5-S6
Figure S9 The Nyquist plots of the catalysts	S6
Figure S10 The cycles of i-t curves for another 60 h	S7
Figure S11 Time optimization results in the synthesis of TBA- $\text{Ti}_3\text{C}_2\text{T}_x$	S7
Figure S12 The calibration of 3.5 M Ag/AgCl electrode with respect to RHE	S8
Figure S13 The LSV curve of TBA- $\text{Ti}_3\text{C}_2\text{T}_x$ -Pt-20 synthesized with short time	S8
Figure S14. HRTEM of TBA- $\text{Ti}_3\text{C}_2\text{T}_x$ -Pt-20 before and after cycled for 80 h	S8
Figure S15. Polarization curves of the catalysts in alkaline and neutral solutions	S9
Table S1 Contents of Pt in the catalysts determined by ICP-OES	S9

Supplementary Figures

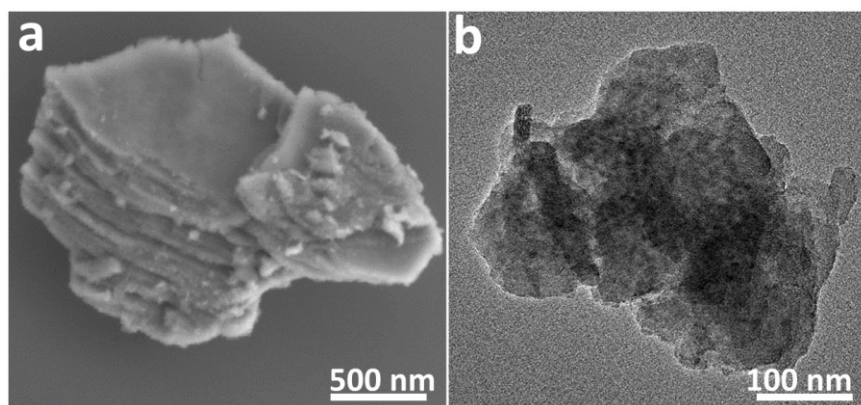


Figure S1. Morphological characterization of $\text{Ti}_3\text{C}_2\text{T}_x$. (a) the SEM and (b) TEM characterization of $\text{Ti}_3\text{C}_2\text{T}_x$.

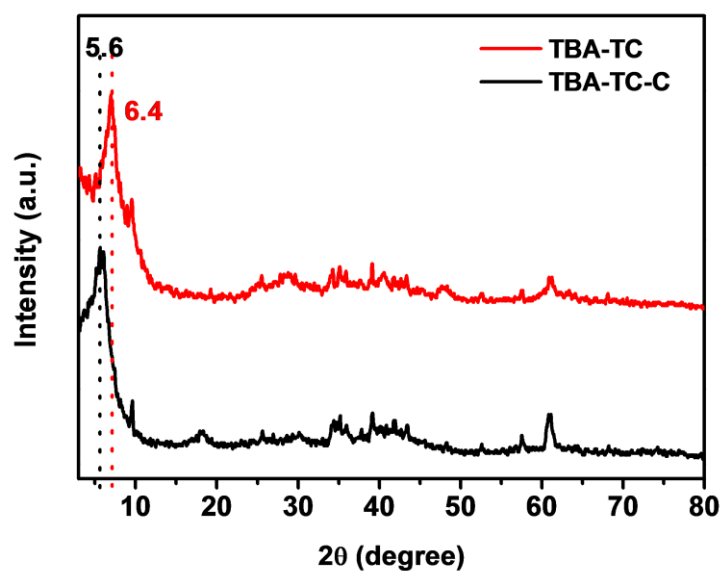


Figure S2. XRD patterns of TBA- $\text{Ti}_3\text{C}_2\text{T}_x$ treated with 25 wt% (black) and 2.5 wt% (red) TBAOH solutions.

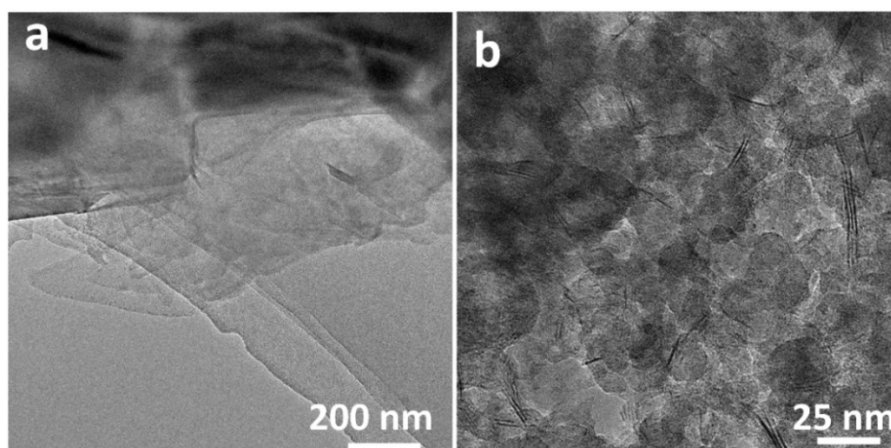


Figure S3. TEM characterization of D-Ti₃C₂T_x. (a) TEM image of. (b) HRTEM image of D-Ti₃C₂T_x indicating the layers (2-3 layers).

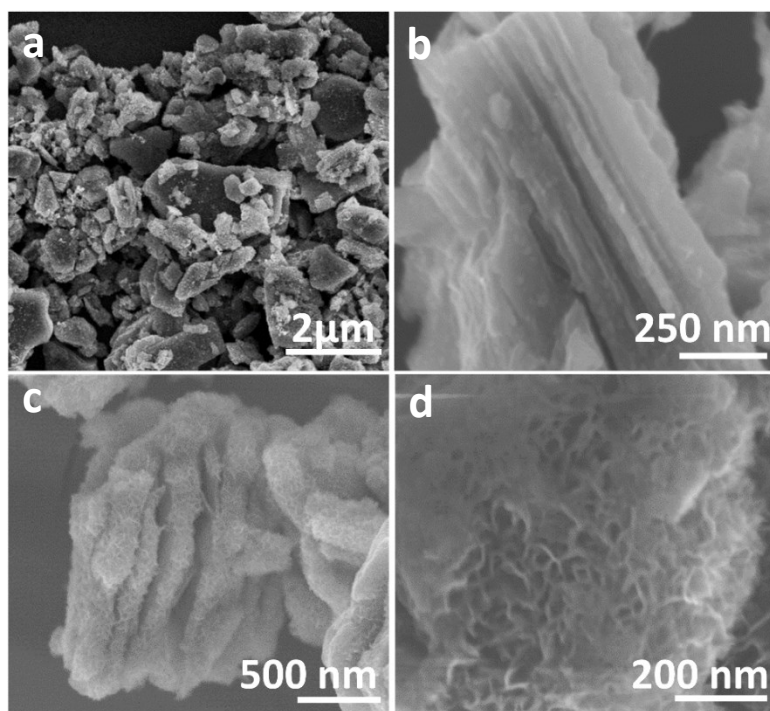


Figure S4. Morphological characterization of TBA-Ti₃C₂T_x obtained in different TBAOH concentration. (a) SEM images of TBA-Ti₃C₂T_x-c. (b) The enlarged image of (a). (c) SEM images of TBA-Ti₃C₂T_x. (d) The enlarged image of (c).

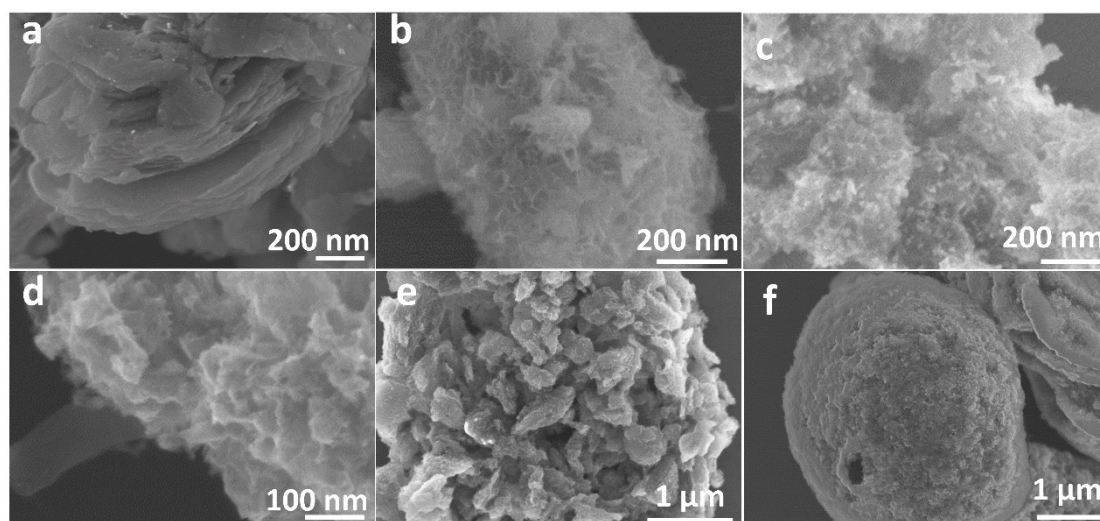


Figure S5. Morphological characterization of the supports and the catalysts. (a) SEM images of K-Ti₃C₂T_x (b) SEM image of TBA-Ti₃C₂T_x. (c) The morphology of TBA-Ti₃C₂T_x-Pt with

the reduction of NaBH_4 . (d) The morphology of $\text{D-Ti}_3\text{C}_2\text{T}_x\text{-Pt}$ with the reduction of NaBH_4 . (e) The morphology of $\text{TBA-Ti}_3\text{C}_2\text{T}_x\text{-Pt}$ with the method of UV-induced reduction. (f) The morphology of $\text{D-Ti}_3\text{C}_2\text{T}_x\text{-Pt}$ with the method of UV-induced reduction.

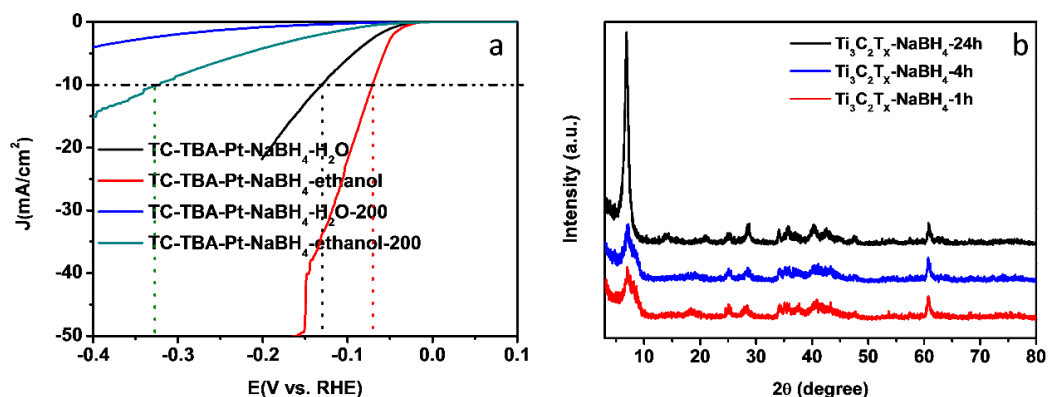


Figure S6. Optimization results of the (a) solvent and (b) reaction time in the reduction process by NaBH_4 . The reduction time and solvent are optimized with a perfect time of 4 h in aqueous solution.

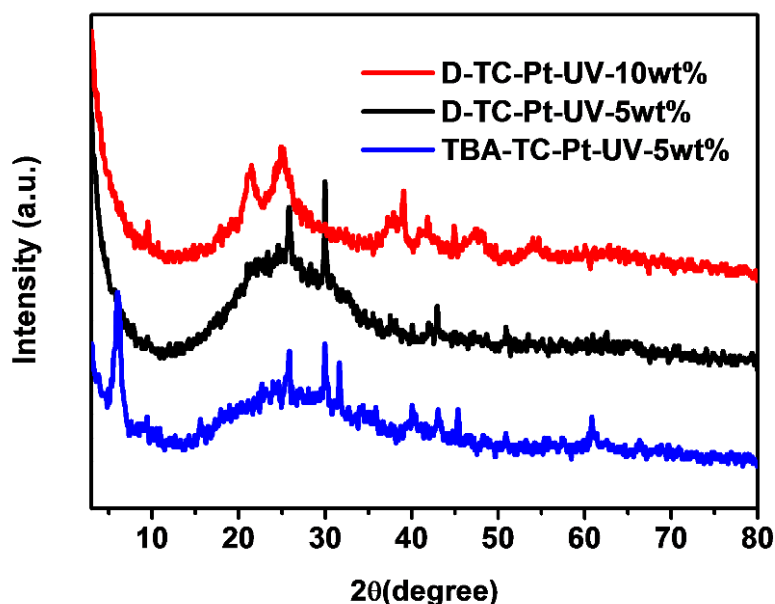
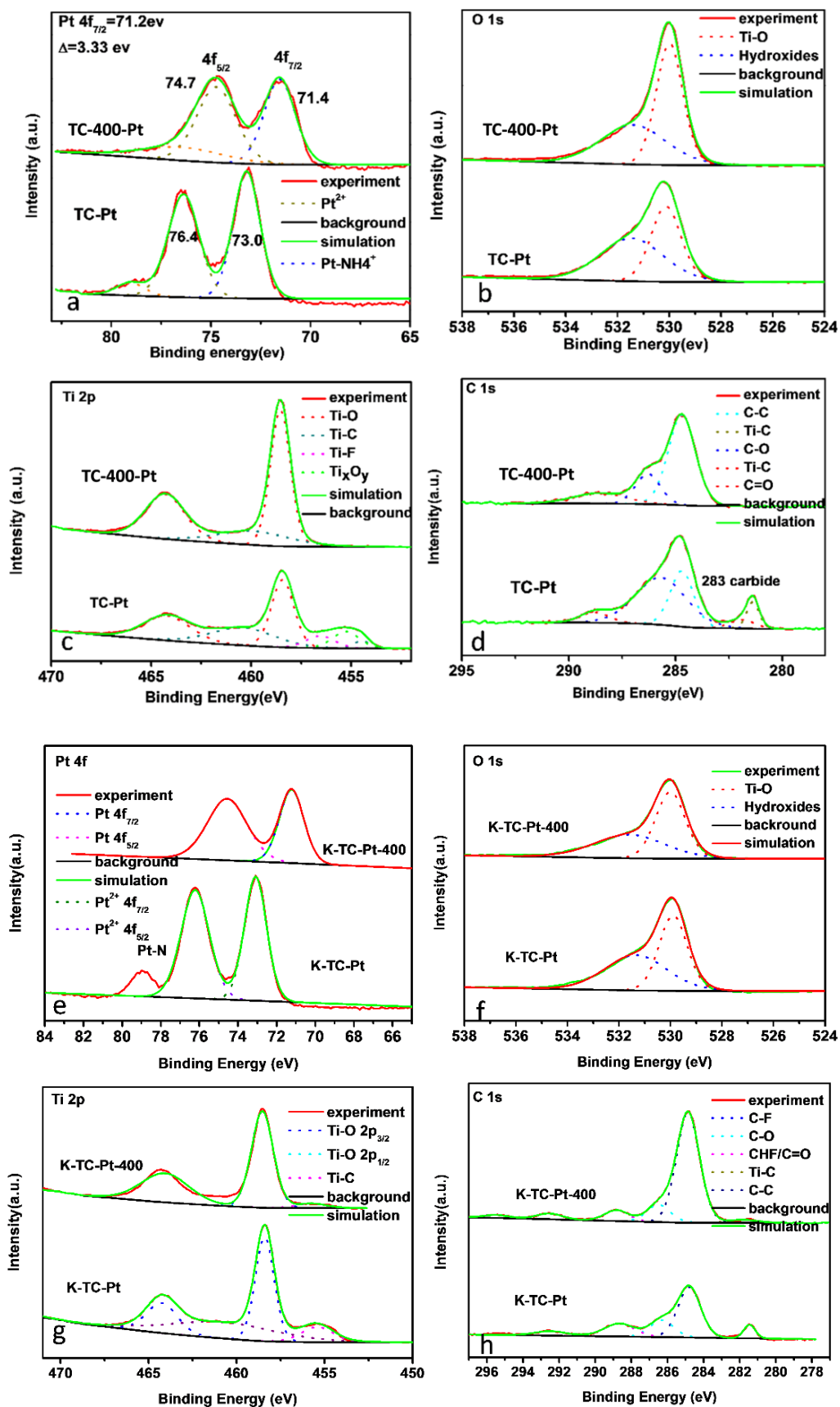


Figure S7. XRD patterns of $\text{TBA-Ti}_3\text{C}_2\text{T}_x\text{-Pt}$ (blue) and $\text{D-Ti}_3\text{C}_2\text{T}_x\text{-Pt}$ (red and black) obtained by the UV-induced method.



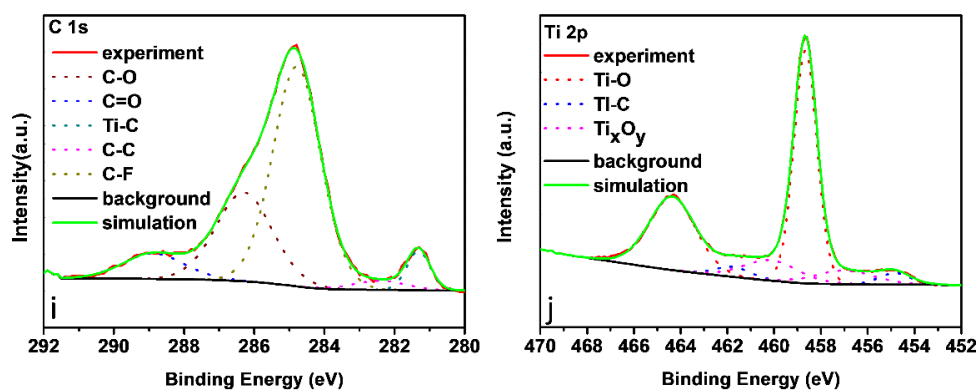


Figure S8. XPS results of the catalysts. XPS of the (a) Pt 4f, (b) O 1s, (c) Ti 2p, (d) C 1s spectra of the $\text{Ti}_3\text{C}_2\text{T}_x\text{-400-Pt-20}$ and $\text{Ti}_3\text{C}_2\text{T}_x\text{-Pt-20}$. XPS results of (e) Pt 4f, (f) O 1s, (g) Ti 2p, (h) C 1s of $\text{K-Ti}_3\text{C}_2\text{T}_x\text{-Pt-20-400}$ and $\text{K-Ti}_3\text{C}_2\text{T}_x\text{-Pt-20}$. (I, j) XPS of the C 1s and Ti 2p spectra of $\text{TBA-Ti}_3\text{C}_2\text{T}_x\text{-Pt-20}$.

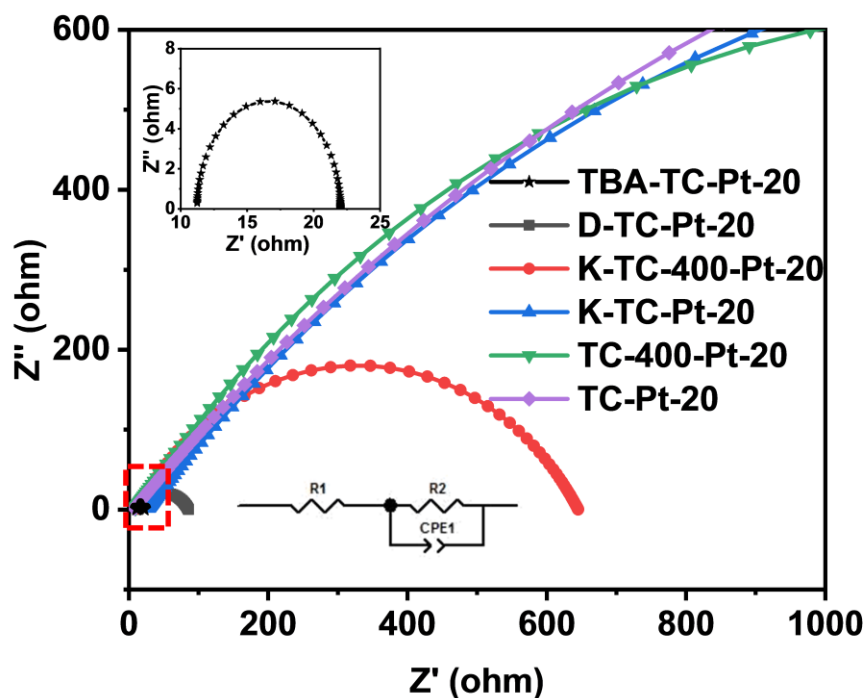


Figure S9. The Nyquist plots of the corresponding samples measured at a voltage of -60 mV (vs. the RHE) over the frequency range from 100 kHz to 0.1Hz with the amplitude of 5 mV in 0.5 M H_2SO_4 .

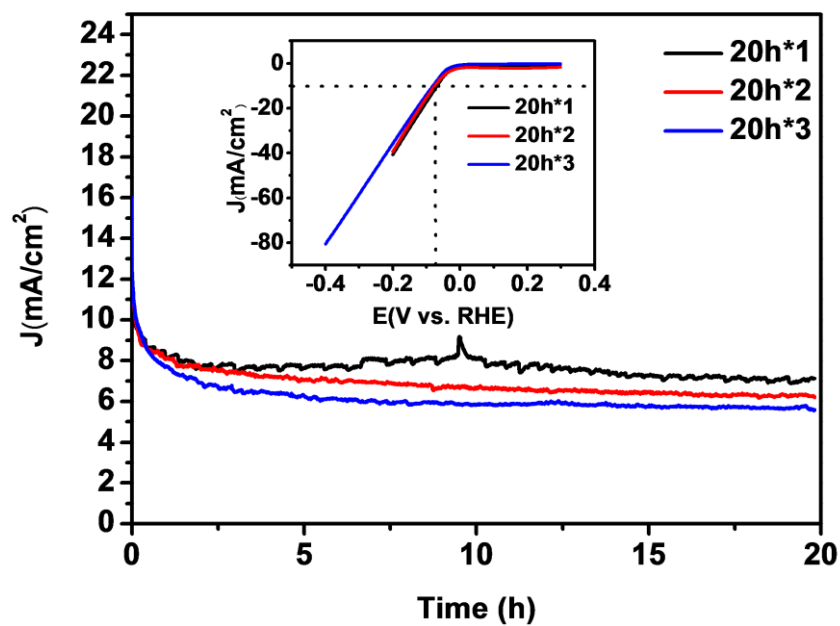


Figure S10. The cycles of i-t curves for another 60 h (the total time is 80 h) and the inset is the polarization curves after the corresponding i-t test.

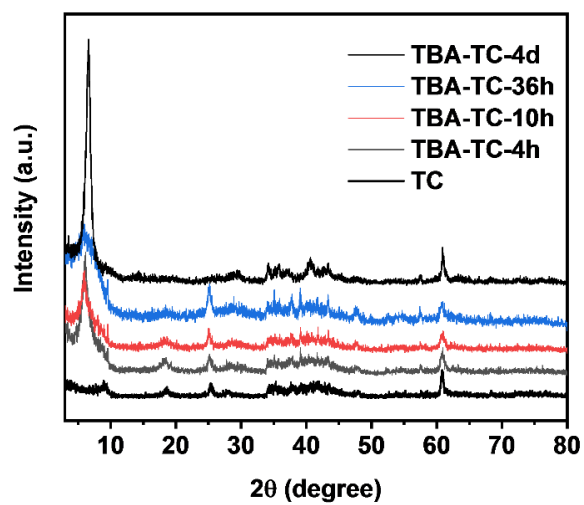


Figure S11. Time optimization results in the synthesis of TBA- $\text{Ti}_3\text{C}_2\text{T}_x$

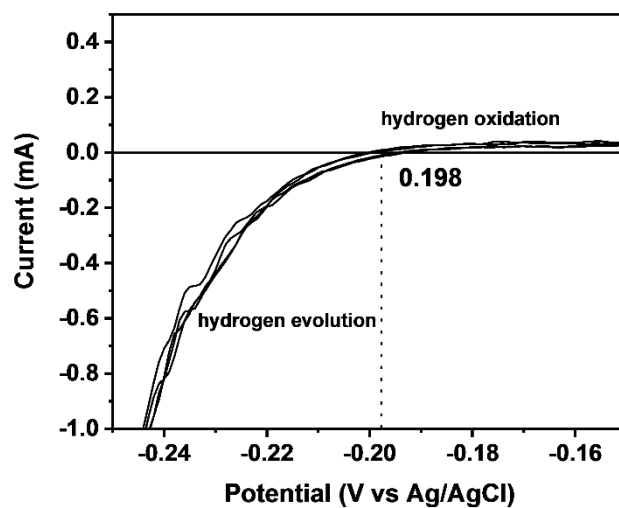


Figure S12. The calibration of 3.5 M Ag/AgCl electrode with respect to reversible hydrogen electrode

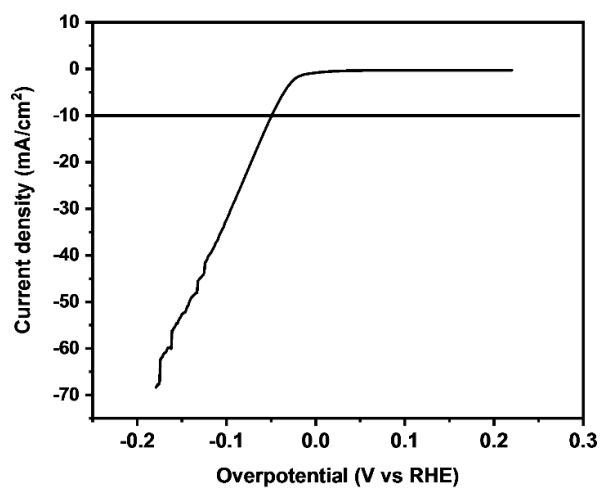


Figure S13. The LSV curve of TBA-Ti₃C₂T_x-Pt-20 synthesized with short time (12h)

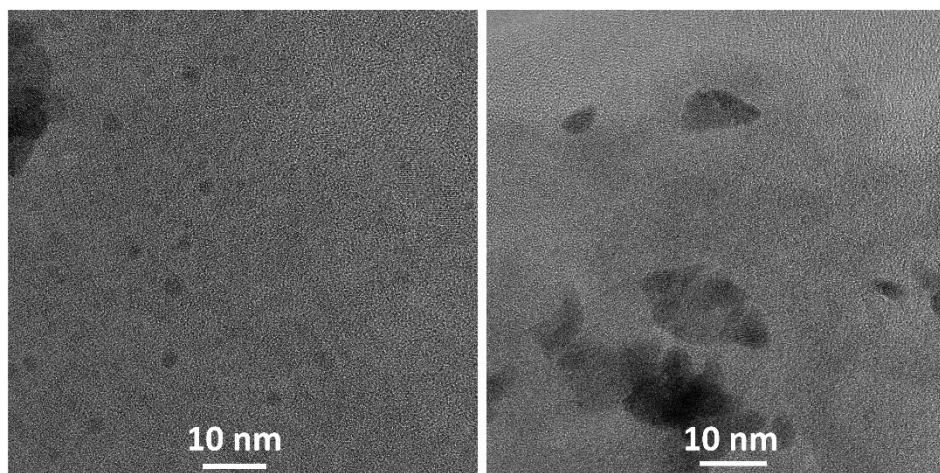


Figure S14. HRTEM of TBA-Ti₃C₂T_x-Pt-20 before (left) and after (right) cycled for 80 h

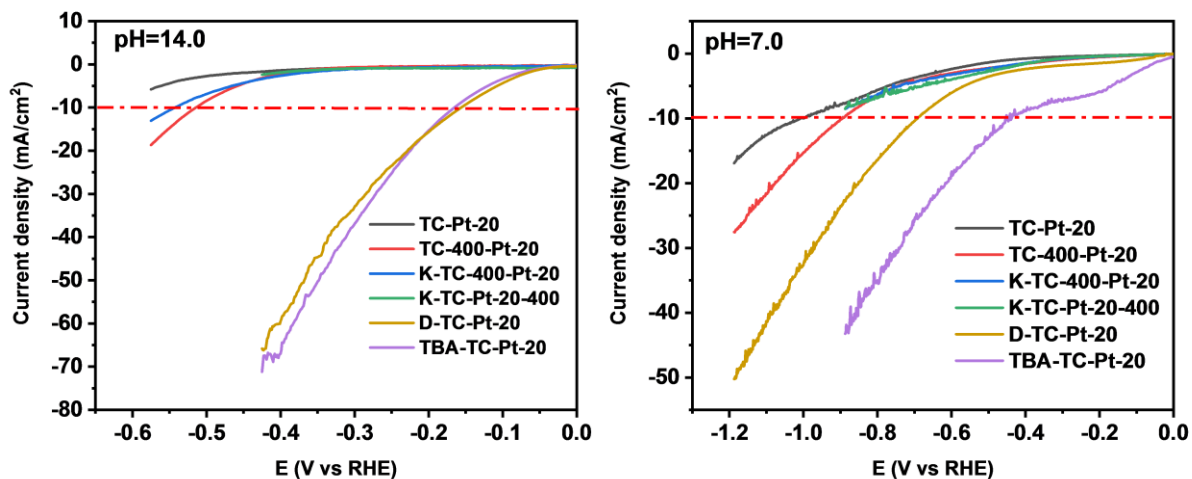


Figure S15. Polarization curves of Pt deposited on the supports in 1M KOH (left) and 0.1 M PBS solutions (right).

Table S1. Contents of Pt in the catalysts determined by ICP-OES

Samples	Pt content (wt%)	Pt NPs size*
TC-400-Pt-20	2.3	--
K-TC-400-Pt-20	0.67	--
K-TC-Pt-20-400	1.15	--
D-TC-Pt-20	0.76	6.4 nm
TBA-TC-Pt-20	1.2	9.4 nm
TBA-TC-Pt-10	1.0	8.4 nm
TBA-TC-Pt-5	0.8	7.3 nm
TBA-TC-Pt-2	0.4	--
TBA-TC-Pt-1	0.4	--

* Pt NPs size was calculated by scherrer formula with the XRD data.